

# Seismic stratigraphy of the flexural moat flanking the Hawaiian Islands

U. S. ten Brink & A. B. Watts

Lamont-Doherty Geological Observatory, and  
Department of Geological Sciences of Columbia University,  
Palisades, New York 10964, USA

The elastic thickness of oceanic lithosphere, based on flexure studies in the region of surface loads, is two to three times smaller than its seismic thickness<sup>1</sup>. Thus, as a load ages, the thickness of the mechanically supportive part of the lithosphere must decrease from its short-term (seismic?) thickness to its long-term mechanical thickness. Extrapolation of data from experimental rock mechanics suggests that thinning occurs by brittle failure in the uppermost part of the lithosphere and thermally activated creep in its lower part<sup>2</sup>. Modelling shows that for load ages less than about 1 Myr, flexural moats change shape and the peripheral bulges migrate in towards the load<sup>3</sup>. These transient changes in flexure are best manifest, we believe, in the stratigraphical sequences that infill flexural moats. The largest thicknesses of sediments occur in moats flanking orogenic belts<sup>4,5</sup>. However, the stratigraphical record in these basins is complicated by the effects of compaction, sub-aerial erosion and sea-level changes, and by the fact that the loading history extends over very long periods of time. Here we describe a multichannel seismic reflection profile across a flexural moat flanking the volcanic load of Oahu in the Hawaiian Islands. The advantages of Oahu are that it is located in the interior of a plate, the load is 2.7 Myr old and formed within 1 Myr<sup>6</sup>, and the flexural moat was not significantly affected by sea-level changes and erosion. We show that the observed stratigraphical patterns cannot be explained by changes in material

influx, load distribution, and rapid relaxation of the lithosphere to its long-term mechanical thickness. Rather, the observed patterns suggest a prolonged relaxation (>1 Myr) due to either local or regional re-heating of the lithosphere. This re-heating has important implications for the relationship between elastic thickness and age of the lithosphere at the time of loadings.

Figure 1 shows common mid-point (CMP) multichannel seismic reflection line 314 of the flexural moat NNE of Oahu, Hawaii. Individual traces were demuxed, gathered and stacked in 50-m bins<sup>7</sup>. Predictive deconvolution was applied after stacking and the data were bandpass filtered (6–30 Hz). Although only one CMP display is shown in Fig. 1, other types of display have also been considered, such as near-trace plots and variable horizontal exaggeration.

The main feature shown in Fig. 1 is a poorly to well stratified wedge of material which infills the region between the northern flank of Oahu and the peripheral bulge. The upper surface of the wedge (the sea floor) is tilted by about 0.75 s from the crest of the bulge to the moat, corresponding to an increase of about 580 m in sea-floor depth. The lower surface is defined by a tilted discontinuous diffractive reflector, similar in character to reflectors associated with the top of the oceanic crust<sup>8</sup>.

Seismic refraction data in the region<sup>7,9</sup> show that the average P-wave velocities in the wedge range from 3.5 to 4.4 km s<sup>-1</sup>. These velocities imply that the wedge thickens to about 2.2 km beneath the flank of the island. The cross-sectional area of the wedge out to a distance of 160 km from the flank of the island is about 157 km<sup>2</sup>, which is 5–10 times larger than would be expected over a similar distance in the deep Pacific ocean basin. Thus, the material comprising the wedge was probably derived from the island and is volcanoclastic in origin. If all the material in the cross-section in Fig. 1 was eroded from Oahu, then its average elevation must have stood about 3–4 km above its present height.

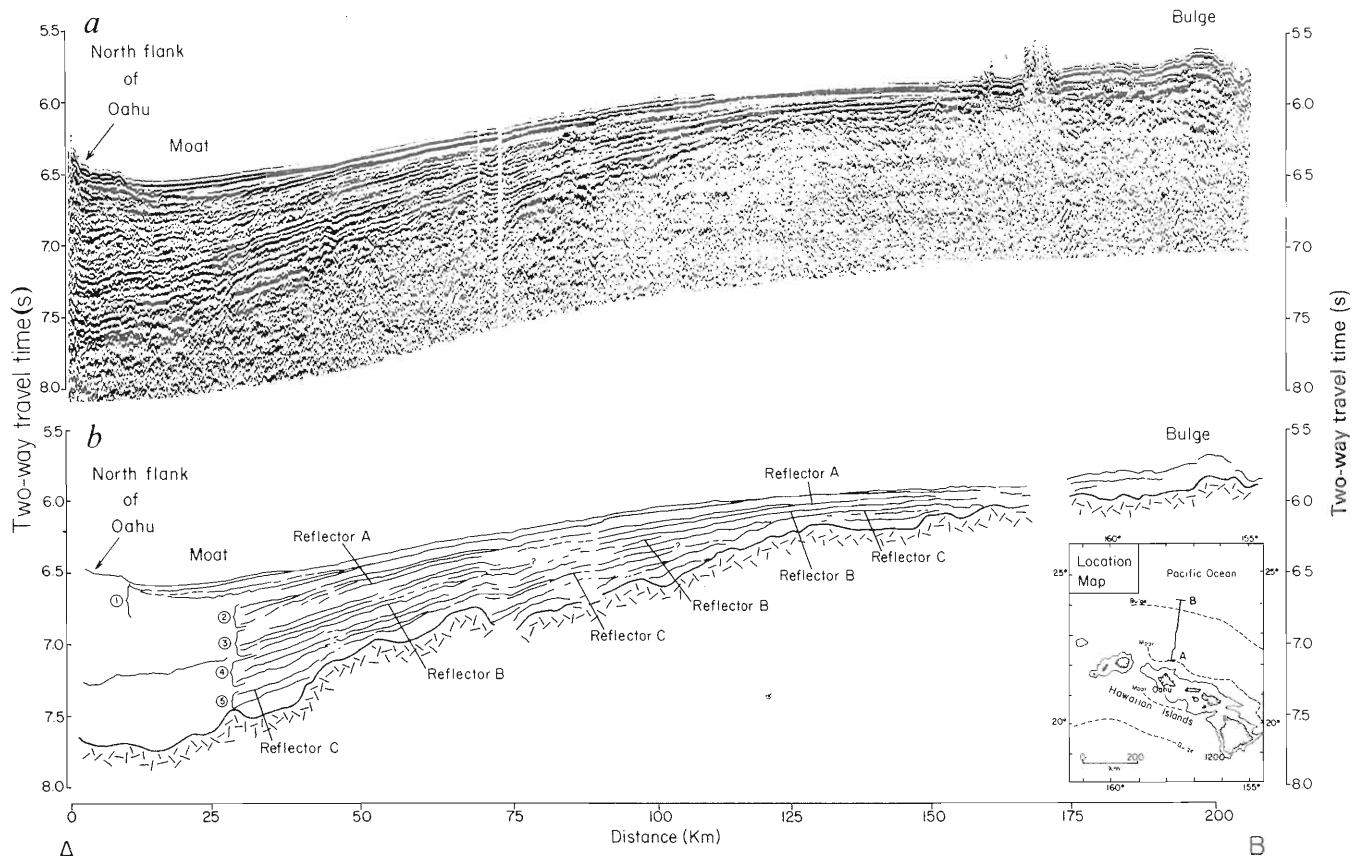


**Fig. 1** Multichannel seismic reflection profile AB of the flexural moat and bulge north of Oahu, Hawaii. *a*, Stacked common mid-point record obtained by RV *Conrad* during August 1982. The receiver consisted of 48 groups of hydrophones on a 3.6-km-long streamer towed behind the ship. The sound source was an airgun array with a total capacity of 2,500 cubic inches. *b*, Line drawing of the stacked record. The numbers represent the units described in the text. The heavy line with hatching indicates the upper surface of the oceanic basement.

The general reflector configuration within the wedge is divergent towards the island. Individual reflectors can be followed laterally for several tens of kilometres, although they often exhibit a hummocky or even broken characteristic. Near the island, reflectors are discontinuous and cannot be traced laterally. Additionally, a velocity inversion analysis<sup>7</sup> shows a high-velocity cap ( $4.5\text{--}5.4\text{ km s}^{-1}$ ) at  $6.7\text{--}7.2\text{ s}$  two-way travel time, suggesting that a basaltic sill or volcanic flow may have been emplaced within the moat infill. In the wedge, seismic reflection patterns of the type normally associated with erosional surfaces<sup>10</sup> do not appear to be present. However, many reflector terminations can be identified in the wedge and are spread out over most of its length.

For purposes of description, we have divided the seismic stratigraphy of the wedge into five principal units (Fig. 1b). Each unit is bounded by a high-amplitude reflector and shows a distinct pattern within it. Unit 5 drapes and infills rough topography of the upper surface of the oceanic crust. It is probable therefore that this unit pre-dates the formation of the flexural moat by the Hawaiian volcanic loads. Unit 4 is bounded at its base by a discontinuous reflector (C, Fig. 1b) and at its top by a high-amplitude reflector (B). Some of the reflectors in

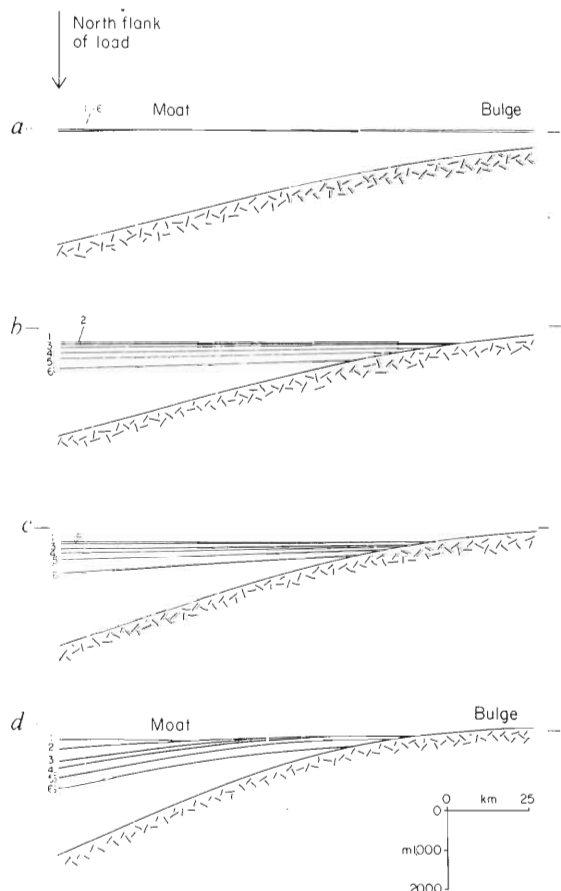


**Fig. 2** Synthetic stratigraphy predicted by a two-dimensional continuous elastic plate model loaded by a load the size of Oahu. The strength of the plate is limited by the YSE and the relaxation process is described in six time steps. *a*, Infill to pre-deformational surface. Time step, 0.5 Myr. Ductile flow given by the power law and Dorn law with activation energy =  $510\text{ kJ mol}^{-1}$  and other parameters as defined by Bodine *et al.*<sup>3</sup>. *b*, Same as *a* except for infill to a variable level. *c*, Same as *b* except that ductile flow is given by temperature-dependent newtonian viscosity with activation energy =  $170\text{ kJ mol}^{-1}$  and basal viscosity of  $10^{18}\text{--}10^{20}\text{ Pa s}$  (ref. 15). When expressed in power law form, the parameters are stress power = 1 and pre-stress term =  $1.16 \times 10^{-8}\text{--}1.16 \times 10^{-10}\text{ bar}^{-1}\text{ s}^{-1}$ . *d*, Same as *b* except that the equivalent thermal age of the lithosphere is reduced through time. The parameters used to produce the models are given in Fig. 5a of Watts *et al.*<sup>9</sup> for the load size, load density, infill and mantle density.

unit 4 appear to overstep progressively towards the bulge, although the resolution in this deep unit is poor. The next unit above, 3, is capped by another high-amplitude reflector (A) and clearly shows progressive overstepping from 75 to 160 km. This pattern is reversed in unit 2 in which most of the reflectors offstep progressively towards the islands. The uppermost unit, 1, does not show a preferential direction of overstepping or offstepping. Furthermore, the infilling material 'ponds' close to the flank of the island, with reflector termination at both ends. Hence, the overall stratigraphical pattern is one of migration of reflector terminations towards the bulge in the lower part of the section to migration towards the flank of the island in the upper part, and a random pattern of migration and ponding in the top-most part of the moat infill. We caution, however, that the distance between individual reflectors is close to the limits of the seismic resolution and therefore the exact location and relationship at reflector terminations are not always easy to determine.

We suggest that three principal factors have controlled the reflector patterns in the wedge flanking Oahu: the rate of material influx, temporal and spatial changes in the distribution of the Oahu load, and tectonic movements of the underlying oceanic lithosphere. In order to investigate the role of these different factors, synthetic stratigraphical models have been constructed and compared with the observed seismic section. In the absence of age control, we assume that individual reflectors correspond to chrono-stratigraphical horizons.

A commonly used rheology of the oceanic lithosphere is the yield stress envelope (YSE) model<sup>2</sup>. In this model, the strength of oceanic lithosphere is limited by brittle failure in the form of Byerlee's law in the upper part of the lithosphere and by ductile flow in the form of the power law ( $n=3$ ) and the Dorn law in the lower part.

Figure 2a shows the relaxation of a two-dimensional elastic plate caused by a distributed load the size of Oahu. The strength of the plate is limited by the YSE, and the elastic thickness varies laterally because of flexure-induced stress concentrations. We describe the relaxation process in six time steps of 0.5 Myr duration, which sums to the approximate age of Oahu<sup>6</sup>. Within each time step, the flexure was calculated by loading a thin elastic plate and iterating until convergence was achieved for the corresponding YSE. The strain rate in the ductile flow law was computed for each time step assuming the empirical relationship<sup>3</sup> between strain and time. A synthetic stratigraphy was constructed by successively adding the differences of individual flexure curves. At each time step, we assumed that the material filling the flexural moat was deposited horizontally and that it infilled to the pre-deformational surface. A comparison between Fig. 1 and Fig. 2a shows poor agreement between the synthetic and the observed section.

In order to fit the observed section better, the parameters in the simple model shown in Fig. 2a were varied. We first investigated changes in the material influx to the moat by varying the level of infill for each time step. We assumed a decreasing rate of material influx—consistent with the decrease in average elevation of the Hawaiian Islands with time. Figure 2b shows an example where infill level rises with time in such a way that the final height of the infill is 370 m below the pre-deformational surface. A limit to the moat infill is in accord with the observed differences in sea-floor depths between the bulge and the moat (Fig. 1). The stratigraphical pattern produced in the model in Fig. 2b is one of progressive overstepping towards the bulge and little or no divergence of individual horizons towards the load. Other variations in the rate of material influx produced similar stratigraphical patterns. Decreasing the six time steps to 0.075 Myr (total of 0.45 Myr) did not alter the stratigraphical pattern significantly. Any further reduction in the time step would imply an unreasonably high accumulation rate in the moat. A comparison of Fig. 2b with the observed section shows that while a variable-infill model could explain the pattern of overstepping shown in units 1 and 2, it cannot account for either



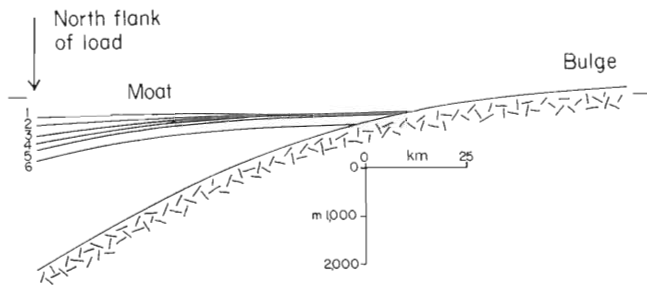


**Fig. 3** Synthetic stratigraphy produced by using a thin-elastic plate model and varying the rigidity of the plate through time. Load, time steps and other parameters are as in Fig. 2. In the model, the rigidity is decreased from a normal value of  $5 \times 10^{30}$  (elastic thickness,  $T_e = 30$  km) to a minimum of  $10^{29}$  dyn cm ( $T_e = 5$  km) beneath the load. The elastic thickness is decreased linearly towards the centre of the load and the width of the weakened zone increases with time step to a maximum value 100 km either side of the load.

the patterns in the upper units or the overall tilting of individual reflectors.

The synthetic stratigraphy shown in Fig. 2b could not be significantly altered by changing the width of the load or the form of the ductile flow law. An increase in the load width, for example, would only enhance the pattern of overstepping seen in Fig. 2b. Moreover, the use of a temperature-dependent newtonian viscosity expressed as a power law does not significantly alter the overall pattern in the moat (Fig. 2c).

We found that the stratigraphical patterns observed in the moat could only be explained by a model in which there was a further reduction in plate rigidity with time. This reduction was achieved by perturbing the oceanic geotherm and hence altering the depth at which material responds to loads by thermally activated creep. Figure 2d shows a flexure model with similar parameters as in the model in Fig. 2b except for the choice of the oceanic geotherm. In Fig. 2b, the geotherm is set to correspond to that of 80-Myr-old sea floor and does not change with time. In Fig. 2d, the geotherm is the same for the first two steps of loading as in Fig. 2b, and is subsequently progressively elevated corresponding to a decrease in effective thermal age with time. At the final step of loading, the geotherm corresponds to about 44-Myr-old sea floor.

In contrast to the previously discussed models, the model in Fig. 2d compares well with the observed stratigraphical cross-section in Fig. 1. Specifically, the model shows a divergent pattern of horizons toward the load, a tilted sea floor, and stratigraphical patterns which closely resemble the succession of units in Fig. 1.

The observed section could also be simulated using a thin continuous elastic plate model and progressively decreasing its rigidity over successively wider areas with each load step. The resulting synthetic stratigraphy (Fig. 3) compares reasonably well with the observed profile. We found the model pattern, however, to be extremely sensitive to the spatial and temporal changes in the rigidities that were assumed.

Figures 2d and 3 show that in order to explain the observed stratigraphical patterns, it is necessary to weaken the plate progressively over a longer period of time ( $\sim 1$  Myr or more) than would be predicted by the YSE. According to the YSE, the greatest reduction in rigidity occurs over relatively short times ( $\sim 10^4$ – $10^5$  yr). Moreover, the rate of subsidence is small after  $10^4$ – $10^5$  yr, producing stratigraphical patterns of the type shown in Fig. 2a–c. In order to account for the divergent reflectors in the observed profile, a higher rate of subsidence is required for longer times ( $\sim 1$  Myr). In the model in Fig. 2d, the subsidence rate at the edge of the load is persistent at about  $0.20 \text{ mm yr}^{-1}$  for the past 2.5 Myr. Beneath the load, the rate increases from  $0.25$  to  $1.00 \text{ mm yr}^{-1}$  during the same period. Although Moore<sup>11</sup> suggested, on the basis of tide-gauge records,

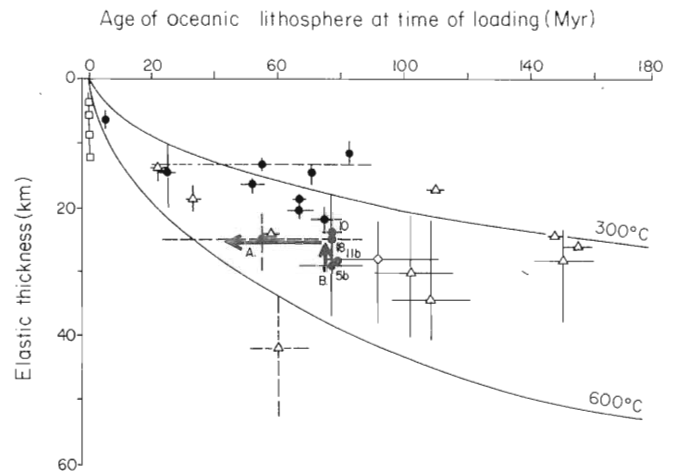


**Fig. 4** Plot of the elastic thickness of the lithosphere against age of the lithosphere at the time of loading. ●, Seamount loads; △, trenches; □, mid-oceanic ridge crest topography. Numbered circles are various estimates<sup>2,9</sup> of elastic thicknesses for the Hawaiian Islands. Arrows represent: A, shift of elastic thickness to a younger apparent age due to regional re-heating, B, shift of elastic thickness to an average lower value due to local thermal perturbation. Solid lines are the 300 °C and 600 °C oceanic isotherms based on a cooling plate model.

that Oahu is stable relative to the west coast of the United States, Gregory and Kroenke<sup>12</sup> pointed out the existence of carbonate reefs on the southern shelf of Oahu whose depth ( $> 500$  m) could not be explained by eustatic sea-level change.

A possible explanation for a sustained weakening of the lithosphere is re-heating and thinning of the lithosphere in the vicinity of the Hawaiian 'hot-spot'. Detrick and Crough<sup>13</sup> suggested, on the basis of bathymetric data, that 80-Myr-old oceanic lithosphere in the vicinity of Hawaii was re-set over a broad region to a thermal age of 30 Myr in about 5 Myr following the initial heating event. The model in Fig. 2d, in which the geotherm is perturbed to an equivalent age of 44 Myr after about 3 Myr, is in accord with this suggestion. It may also be possible, as Fig. 3 shows, to explain the observed section by a progressive broadening of a zone of weakness in the lithosphere beneath the load. This could have resulted from continued penetration of intrusive material into the portion of the plate that behaves elastically on long timescales. The form of this intrusion is unknown, but it may correspond to the deep crustal sill complex, identified in the recent seismic study<sup>9</sup> in the vicinity of Oahu.

The inferred perturbation of the oceanic geotherm associated with volcano building has important implications for the relationship between elastic thickness and age of oceanic lithosphere at the time of loading<sup>14</sup>. According to this relationship, the elastic thickness increases with age, following the depth to the 450 °C oceanic isotherm. However, if thermal perturbations of the ocean geotherm occur, then some modifications of this relationship is expected. Figure 4 shows that if the regional geotherm is perturbed in the manner described here, then the plotted position of the elastic thickness at Oahu would have to be shifted from its age at the time of loading ( $\sim 80$  Myr) to its equivalent thermal age (44 Myr). In this case, the Oahu value will better fit the depth to the 550 °C. If, on the other hand, a local re-heating occurs and elastic thickness varies laterally (Fig. 3), then the observed average elastic thickness will shift towards lower values.

The seismic reflection profile described here is, we believe, the first that was collected in a flexural moat flanking a large volcanic island in the interior of a plate. In order to understand fully the thermo-mechanical setting of large volcanic loads, more data will be required in flexural moats. It will be of particular importance to document the age relationships of the stratigraphical units in the moat and the subsidence history of the

island by drilling. These data, together with the development of more refined models, will significantly advance our understanding of the mechanics of flexure.

Received 4 April; accepted 2 August 1985.

1. Watts, A. B., Bodine, J. H. & Steckler, M. S. *J. geophys. Res.* **85**, 6369–6376 (1980).
2. Goetze, C. & Evans, B. *Geophys. J. R. astr. Soc.* **59**, 463–478 (1979).
3. Bodine, J. H., Steckler, M. S. & Watts, A. B. *J. geophys. Res.* **86**, 3695–3707 (1981).
4. Jordan, T. E. *Am. Ass. Petrol. geol. Bull.* **65**, 2506–2520 (1981).
5. Quinlan, G. M. & Beaumont, C. *Can. Earth Sci.* **21**, 973–996 (1984).
6. Sen, G. *Earth planet Sci. Lett.* **62**, 215–228 (1983).
7. Brocher, T. M. & ten Brink, U. S. *J. geophys. Res.* (submitted).
8. Ewing, J. I., Ewing, M. & Aitken, T. *Am. geophys. Un. Geophys. Mon.* **12**, 147–173 (1968).
9. Watts, A. B., ten Brink, U. S., Buhl, P. & Brocher, T. M. *Nature* **315**, 105–111 (1985).
10. Mitchum, R. M. Jr, Vail, P. R. & Thompson, S. III *Am. Ass. Petrol. geol. Mem.* **26**, 53–81 (1977).
11. Moore, J. G. *Bull. Volcanol.* **34**, 562–576 (1970).
12. Gregory, A. E. & Kroenke, L. W. *Am. Ass. Petrol. geol. Bull.* **66**, 843–859 (1982).
13. Detrick, R. S. & Crough, S. T. *J. geophys. Res.* **83**, 1236–1244 (1978).
14. Watts, A. B. *J. geophys. Res.* **83**, 5989–6004 (1978).
15. Courtney, R. C. & Beaumont, C. *Nature* **305**, 201–204 (1983).

We thank M. Steckler and G. Mountain for special assistance. This work was supported by NSF grant OCE-82-11704 and Lamont-Doherty Contribution 3885.